Anal Bioanal Chem
DOI 10.1007/s00216-016-9441-z

RESEARCH PAPER

A self-assembling RNA aptamer-based nanoparticle sensor for fluorometric detection of Neomycin B in milk

Kai Ling[1,2,3] · **Hongyan Jiang**[4] · **Linlin Zhang**[5] · **Yang Li**[1,2] · **Lu Yang**[1,2] · **Chen Qiu**[1] · **Fu-Rong Li**[1,2]

Received: 28 November 2015 / Revised: 30 January 2016 / Accepted: 22 February 2016

Abstract To date, there are few reports regarding the development of RNA aptamer-based biosensors for the detection of small molecules. The possible reason is attributed to the weak nuclease resistance of RNA in biological environments. In this study, we have developed an RNA aptamer-based gold nanoparticle (AuNP) sensor for fluorometric detection of Neomycin B in milk. This aptasensor depends on the self-assembly of the RNA aptamer/Neomycin B complex and fluorescence quenching by AuNPs. This biosensor exhibited a low detection limit of 0.01 μM, with a linear dynamic range from 0.1 to 10 μM in milk, and a good selectivity toward Neomycin B. Specifically, because of the shorter RNA fragments and the nuclease inhibition ability of the RNA-modified AuNPs, the RNA sequences remained stable during the experiments. This work will serve as an example for the development of novel biosensors based on RNA aptamers.

Keywords Gold nanoparticle · RNA aptamer · Aptasensor · Self-assembly · Neomycin B

Kai Ling, Hongyan Jiang and Linlin Zhang contributed equally to this work.

Electronic supplementary material The online version of this article (doi:10.1007/s00216-016-9441-z) contains supplementary material, which is available to authorized users.

✉ Fu-Rong Li
frli62@163.com

[1] The Second Clinical Medical College (Shenzhen People's Hospital), Jinan University, No. 1017 Dongmen North Road, Shenzhen 518020, China

[2] School of Medicine, Jinan University, Guangzhou 510632, China

[3] Shenzhen Institute of Geriatrics, Shenzhen 518020, China

[4] Institute of Biomedical Engineering, Key Laboratory of Biomedical Material of Tianjin, Chinese Academy of Medical Sciences & Peking Union Medical College, 236 Baidi Road Nankai District, Tianjin, Tianjin 300192, China

[5] Department of Nuclear Medicine, Xinhua Hospital, School of Medicine, Shanghai Jiaotong University, 227 South Chongqing Road, Shanghai 200092, China

Introduction

Aptamers are oligonucleotide or peptide molecules that can bind to a wide range of target molecules with high affinity and specificity [1, 2]. Like antibodies, aptamers are able to fold into well-defined, three-dimensional (3D) structures that facilitate binding of the corresponding targets. Therefore, aptamers are beginning to rival antibodies as sensors in a number of applications, such as environmental monitoring and medical diagnostics [3, 4]. In comparison with antibodies, aptamers are relatively easy to obtain, more stable toward biodegradation, and less vulnerable to denaturation [5]. Due to their distinct physical and chemical attributes, gold nanoparticles (AuNPs) have been conjugated with aptamers for the fabrication of novel chemical and biological nanosensors, which transforms the aptamer-binding events into physically detectable signals [5].

To date, many aptasensors have been comprised of DNA aptamers as the recognition element, because of their relative stability in biological environments as compared to their counterparts. However, most (70 %) reported aptamers are composed of RNA [6]. Based on existing evidence, the presence of a 2′-OH group and non-Watson-Crick base pairing allow RNA aptamers to fold into more diverse 3D structures than DNA [7]. Many small molecules interact with RNA better than with DNA [8]. Therefore, it is more advantageous to utilize RNA aptamers as sensing tools in the detection of small molecules than DNA-based aptasensors. At the same time, the

Published online: 04 March 2016

nuclease resistance of RNA-aptasensors must be increased in biological environments. Substitutions of the 2′-OH functional group on RNA with 2′-fluoro, 2′-amino, or 2′-*O*-methoxy motifs, and/or replacements of the phosphodiester backbone with boranophosphate or phosphorothioate moieties are the most common modifications aimed at increasing nuclease resistance [7]. Other effective modifications have been based on locked nucleic acid technology [9] or "mirror" RNA sequence structures [10]. Although these modifications prevent digestion of RNA sequences by nucleases, they may result in structural changes to the RNA sequences, which affect the binding affinity [8]. In addition, the above strategies will greatly increase the cost of potential applications.

A 23-mer RNA aptamer that recognizes Neomycin B with high sensitivity and specificity was selected in vitro [11]. As an aminoglycoside antibiotic, Neomycin B has been widely used in veterinary medicine to treat bacterial infections in animals [12]. The presence of Neomycin in animal-derived foods is potentially ototoxic and nephrotoxic to humans [12]. Therefore, in order to protect consumers, it is essential to monitor Neomycin B content in food. The European Union (EU) established maximum residue limits (MRLs) of Neomycin B for edible tissues, fat, milk, and eggs: 500 μg/kg for meat, fat, liver, eggs; 1500 μg/kg (about 2.44 μM) for milk; and 5000 μg/kg for kidney [13]. Therefore, a biosensor will serve well for the purpose of monitoring the drug residue, which possesses a low detection limit (LOD) of 0.01 μM, with a linear dynamic range from 0.1 to 10 μM. Nevertheless, the detection of aminoglycoside antibiotics is a challenging problem because these antibiotics lack distinguishable spectroscopic and chemical properties. Recently, a label-free method was successfully developed for the detection of Neomycin B using a 2′-*O*-methoxy-modified RNA aptamer with surface plasmon resonance and faradaic impedance spectroscopy [8, 14]. However, there are few reports regarding the development of the RNA aptamer-based nanoparticle sensors for the analysis and detection of Neomycin B in biological environments without any chemical modifications.

Therefore, in this study, we constructed an RNA aptamer-based nanoparticle sensor for the fluorometric detection of Neomycin B in milk by using the previously evolved RNA motif [11]. This aptasensor depends on the self-assembly of a bipartite RNA aptamer/Neomycin B complex and fluorescence quenching by AuNPs, which readily responds to Neomycin B in milk within a few minutes.

Materials and methods

Chemicals and materials

All oligonucleotides (HPLC grade) were synthesized and purchased from Takara Biotechnology (Dalian, China). The base sequences were as follows: NEO1 (5′-rGrArArGrUrUrUrArGrUrCrC-$(T)_{15}$-$(A)_{12}$-3′), FAM-labeled NEO1 (5′-FAM-rGrArArGrUrUrUrArGrUrCrC-$(T)_{15}$-$(A)_{12}$-3′), and FAM-labeled NEO2 (5′-FAM-rGrGrArCrUrGrGrGrCrGrA-3′). The lyophilized powders were dissolved in 5 mM HEPES buffer and stored at 4 °C until use. The oligonucleotide concentration was determined by measuring the UV absorbance at 260 nm. Chloroauric acid ($HAuCl_4$), sodium citrate ($C_6H_5Na_3O_7$), Neomycin B sulfate, Paromomycin sulfate, and Kanamycin sulfate were obtained from Sigma-Aldrich (St. Louis, MO, USA). β-Mercaptoethanol (ME) was purchased from Amresco (Solon, OH, USA). Ribonuclease I (RNase I) was purchased from Thermo Scientific (Pittsburgh, PA, USA). All other reagents (analytical grade) were purchased from Sinopharm Chemical Reagent Co., Ltd. (Shanghai, China) and were used as received. Milli-Q ultrapure water (18.2 MΩ cm; Millipore Co., USA) was used throughout the study. All glassware was cleaned using an aqua regia solution ($HCl:HNO_3$ = 3:1, *v*/*v*) and subsequently rinsed with excess Milli-Q water.

Instruments

Ultraviolet-visible (UV-vis) absorption spectra were recorded at room temperature (25 °C), using a Lambda 35 UV/Vis spectrophotometer from PerkinElmer (Waltham, MA, USA). Transmission electron microscope (TEM) images were obtained with a JEM-2010 (Jeol, Ltd., Japan). Fluorescence measurements were recorded with either a Varioskan Flash Multimode Reader (Thermo Electron Co, Waltham, MA, USA) or a QM 40 Spectrofluorometer (Photon Technology International Inc., Lawrenceville, NJ, USA) at room temperature.

AuNP preparation and treatment

AuNPs were prepared using published procedures [15]. Briefly, colloidal AuNPs with an average diameter of 13 nm were prepared by quickly adding 10 mL of 38.8 mM sodium citrate solution into a boiling solution of $HAuCl_4$ (100 mL, 1 mM) with stirring. After the color of the solution changed to deep red, the reaction was heated for an additional 20 min and then cooled to room temperature. Following the preparation, particles were treated with 0.1 % diethylpyrocarbonate (DEPC) for 12 h with stirring, and were subsequently autoclaved at 121 °C for 60 min. The concentration of the AuNPs was about 10 nM, which was determined according to Beer's law using an extinction coefficient of 2.7×10^8 M^{-1} cm^{-1} at 520 nm [16]. The UV-vis absorption spectra and TEM image of the DEPC-treated AuNPs are shown in Electronic Supplementary Material Fig. S1.

RNA-AuNP conjugates

Modification of AuNPs with polyA-tailed RNA sequences was performed, following the previously reported procedure [17]. Briefly, 3 μL of oligonucleotide (NEO1) stock solution (100 μM in 5 mM HEPES buffer, pH 7.6) was added into 200 μL of the as-prepared AuNP solution and mixed briefly via vortex. Citrate buffer (pH 3.0) was added to the AuNP solution to achieve a final citrate concentration of 10 mM. After incubation at room temperature (3 min), the pH of the AuNP solution was adjusted back to neutral by adding 500 mM HEPES buffer to a final HEPES concentration of 30 mM (pH 7.6). The mixture was incubated for another 15 min and then centrifuged at 10,000×*g* for 20 min at 4 °C. The supernatant was removed, and the pellet was washed with 5 mM Tris-HCl buffer to remove free oligonucleotides. The centrifugation and washing procedure was repeated three times to ensure complete removal of free oligonucleotides, and the conjugate was dispersed in 50 mM Tris-HCl buffer (pH 7.4) containing 250 mM NaCl and 5 mM $MgCl_2$ for subsequent use.

The density of the attached polyA-tailed RNA sequences was quantified as previously described [18]. First, the 5′-FAM-labeled NEO1 probe was adsorbed to AuNPs following the protocol outline above. ME was added (final concentration 20 mM) to the oligonucleotide-AuNP solution, which was incubated overnight with shaking at room temperature. The solution was centrifuged at 10,000×*g* for 15 min to release the absorbed probes. The fluorescence (excitation = 492 nm, emission = 518 nm) was measured and converted to the molar concentrations of the probes by interpolation from a standard linear calibration curve, which was prepared with known concentrations of the oligonucleotide with identical buffer pH, ionic strength, and ME concentration.

After ME displacement, the fluorescence of the released sequences was recorded. The intensity of the fluorescence was 46.39 ± 0.27 arbitrary units (AU), which was converted to the molar concentration using the standard curve (see Electronic Supplementary Material Fig. S2). The number of attached RNA sequences per nanoparticle was calculated to be 33.22 ± 0.18. In other words, the overall number of adenines per AuNP was 398.63 ± 2.21. This result is similar to that of a previously published report [18].

The purified RNA (5′-FAM-labeled NEO1) modified AuNPs were dispersed in 50 mM Tris-HCl buffer (pH 7.4) containing 250 mM NaCl and 5 mM $MgCl_2$ and transferred into microcentrifuge tubes (50 μL each with 10 nM AuNPs). At designated time points, the tubes were centrifuged at 10,000×*g* for 20 min at 4 °C and 25 μL of the supernatant was transferred to another tube. After 15 days, the precipitated AuNPs were treated with ME and diluted to 100 μL with a buffer (5 mM HEPES, pH 7.6). The previously collected supernatants were also diluted to 100 μL with the same buffer. The fluorescence of all these supernatant solutions (F_s) and ME-treated AuNPs (F_p) were measured, and the fraction of release was determined to be $2F_s/(F_s + F_p)$.

Fluorometric detection of Neomycin B in milk

Whole milk was diluted 1:5 with 50 mM Tris-HCl buffer (pH 7.4) containing 250 mM NaCl and 5 mM $MgCl_2$ and was subjected to ultracentrifugation at 30,000×*g* for 90 min at 4 °C. Fat and casein were separated (upper and lower layers) from the milk serum (intermediate layer). The serum was collected into vials and stored at 4 °C until use [8, 14].

A 284-μL aliquot of the NEO1-AuNP conjugate solution was added to 6 μL of 100 μM the FAM-labeled NEO2 solution. After complete mixing, a 10-μL aliquot of diluted milk serum sample containing Neomycin B, Paromomycin, and Kanamycin were added to the mixture and then incubated for 10 min at room temperature. Fluorescence measurements of the samples were recorded. For comparison, fluorescence measurements were also performed directly using diluted milk samples.

Ribonuclease resistance studies

A 10-μL aliquot of the 5′-FAM-labeled NEO1-AuNP conjugates was diluted in 80 μL of 50 mM Tris-HCl buffer (pH 7.4) containing 250 mM NaCl and 5 mM $MgCl_2$ and placed in a 96-well fluorescence microplate at 37 °C. After allowing the sample to equilibrate (10 min), 10 μL of RNase I in Tris-HCl buffer (10 units/L) was added. To prevent evaporation, the reaction was covered with 40 μL of mineral oil. The fluorescence of the sample was measured every 120 min for 720 min. To determine the resistance, the fluorescence of aliquots of reaction buffer without enzyme was also measured as a control.

A single aliquot of the centrifuged NEO1-AuNP conjugates was diluted in 90 μL of 50 mM Tris-HCl buffer (pH 7.4) containing 250 mM NaCl and 5 mM $MgCl_2$, and then 10 μL of RNase I in Tris-HCl buffer (10 units/L) was added. The mixture was incubated (0 to 720 min) at 37 °C, and then centrifuged at 10,000×g for 20 min at 4 °C. The absorption spectra of the supernatants were recorded from 240 to 280 nm to evaluate the RNA-specific absorption peak (260 nm) after incubation with RNase I. Absorption spectra of aliquots of the reaction buffer without enzyme were also recorded as controls.

Data analysis

OriginPro 8.0 software (OriginLab, USA) was employed to perform data processing. Each sample measurement was repeated in triplicate, and the data were presented as the mean ± standard deviation.

Results and discussion

A schematic of the design principle for the nanoparticle sensor is shown in Scheme 1a. The RNA aptamer of Neomycin B was split between ribonucleotide A14 (rA14) and rG15 at the end pentaloop region into two shorter half fragments, because shorter RNA chains exhibit fewer interactions with nucleases, which can increase their stability in biological environments [19]. The ligand-binding pocket of the aptamer consists of three rG·rU pairs (rG9·rU21, rG10·rU20, rG11·rU19), a Watson-Crick pair (rC12·rG18), and a non-canonical pair (rG13·rA17) [20]. Furthermore, the looped-out rA16 base acts as a flap over bound Neomycin B [21]. Because the splitting site on the aptamer sequence is outside of the binding pocket, this strategy should not affect the binding properties of the aptamer. One half fragment (NEO1) was connected with a 15 thymidine (T_{15}) spacer, which enabled the appended recognition unit to adopt an upright conformation that favors ligand binding [22], and a polyadenosine (polyA, A_{12}) tail, which acted as an effective anchoring block for preferential adsorption on the surface of AuNPs [18]. The other half fragment (NEO2) was labeled with a fluorescent dye carboxyfluorescein (FAM) at the 5′ end.

Traditional oligonucleotide-AuNP conjugates exploit strong Au−S bonds to assemble thiolated oligonucleotides at the surface of AuNPs [23]. The preparation of the conjugates is rather time-consuming (1–2 days) and inevitably costly [24]. Since vulnerable RNA chains may be degraded during the preparation process, few reports have described the use of RNA-AuNP conjugates in biomedical applications. In this study, we adopted a convenient, rapid, and effective method to prepare RNA-AuNP constructs, through the instantaneous attachment of the polyA tail to AuNPs at pH 3.0 (see Scheme 1b) [25]. This method takes advantage of the high affinity of consecutive adenines toward Au substrates [18] and the protonation of DNA bases at low pH [25]. In addition, oligonucleotide-modified AuNPs are highly stable in

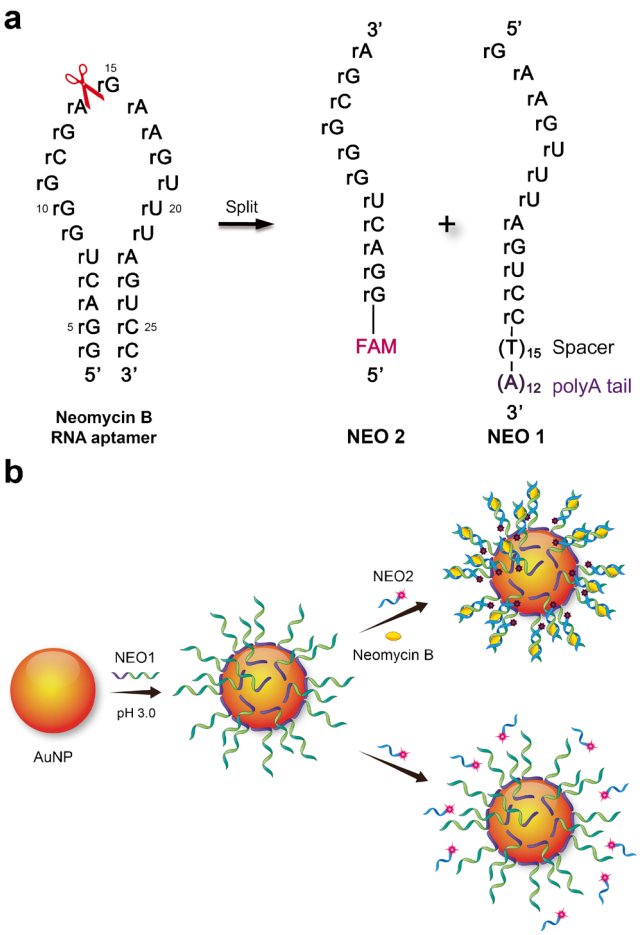

Scheme 1 Schematic illustration of the design principle (**a**) and the sensing mechanism (**b**) of the self-assembling RNA aptamer-based AuNP sensor for the detection of Neomycin B

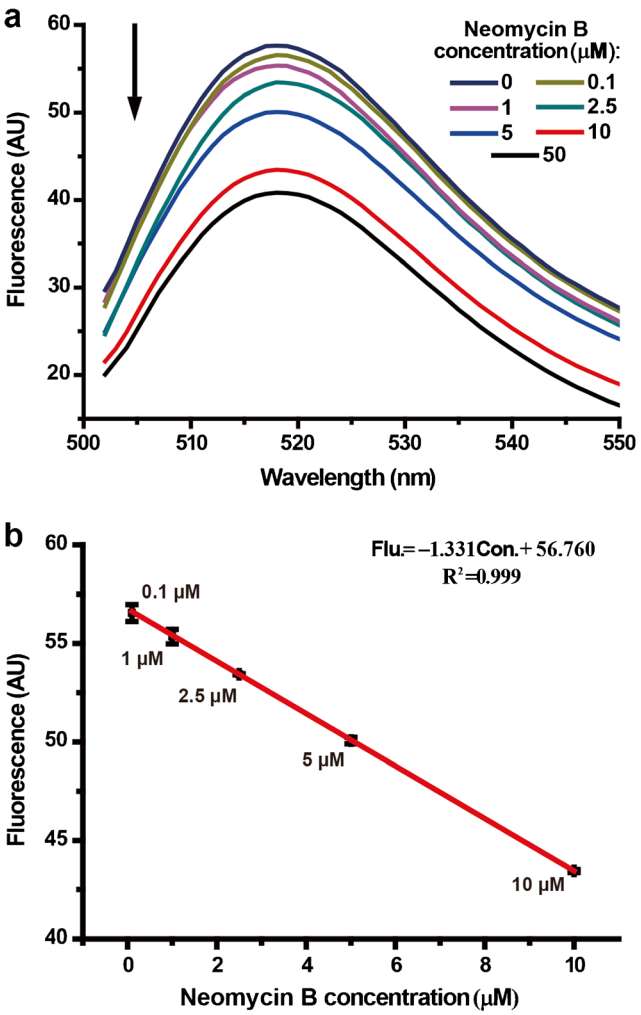

Fig. 1 Neomycin B detection in milk samples. **a** The fluorescence spectra of the self-assembling RNA aptasensor in response to different Neomycin B concentrations in milk samples. **b** The linear relationship between the fluorescence intensity (518 nm) and the Neomycin B concentration (from 0.1 to 10 μM). Data represent mean values and standard deviations from triplicate experiments

biological environments because most nucleases are inhibited by the high local salt concentration around the nanoparticle surface [26]. As shown in Electronic Supplementary Material Fig. S3, if the RNA-modified AuNPs were stored at room temperature (25 °C) in 50 mM Tris-HCl buffer (pH 7.4) containing 250 mM NaCl and 5 mM $MgCl_2$, about 65 % of 5′-FAM-labeled NEO1 dissociated/degraded from the RNA-AuNP conjugates after 15 days. In the same time period, less than 12 % of the nucleic acid sequence dissociated/degraded from the conjugates at 4 °C. Therefore, it is expected that the property of these purified RNA-AuNP conjugates could be maintained for a longer period in a cool environment (4 °C).

Scheme 1b displays the sensing mechanism of the aptasensor in the fluorometric detection of Neomycin B in milk. The bipartite aptamer dissociated in the absence of the ligand. In the presence of Neomycin B, the fragments self-assemble to form defined binding pockets for the free analyte through a conformational change in the secondary structure, leading to the proximity of the AuNPs and FAM, and consequent fluorescence quenching. This nanoparticle aptasensor has a rapid response time and the reaction can occur in complex media. Notably, the fluorescent intensity of the dye changes depending on the concentration of Neomycin B in milk.

As shown in Fig. 1a, the fluorescence intensity decreased as the concentration of Neomycin B increased. This observation suggested that Neomycin B induced the self-assembly of the RNA aptamer-ligand complex on the AuNP surface, which confirmed the feasibility and reliability of the nanosensor design. Additional Neomycin B in the diluted milk serum samples (at least diluted 1:5 with 50 mM Tris-HCl buffer (pH 7.4) containing 250 mM NaCl and 5 mM $MgCl_2$) induced the formation of more self-assembled complexes on the surfaces of the AuNPs, which prompted a higher degree of fluorescence quenching. The dilution of milk serum

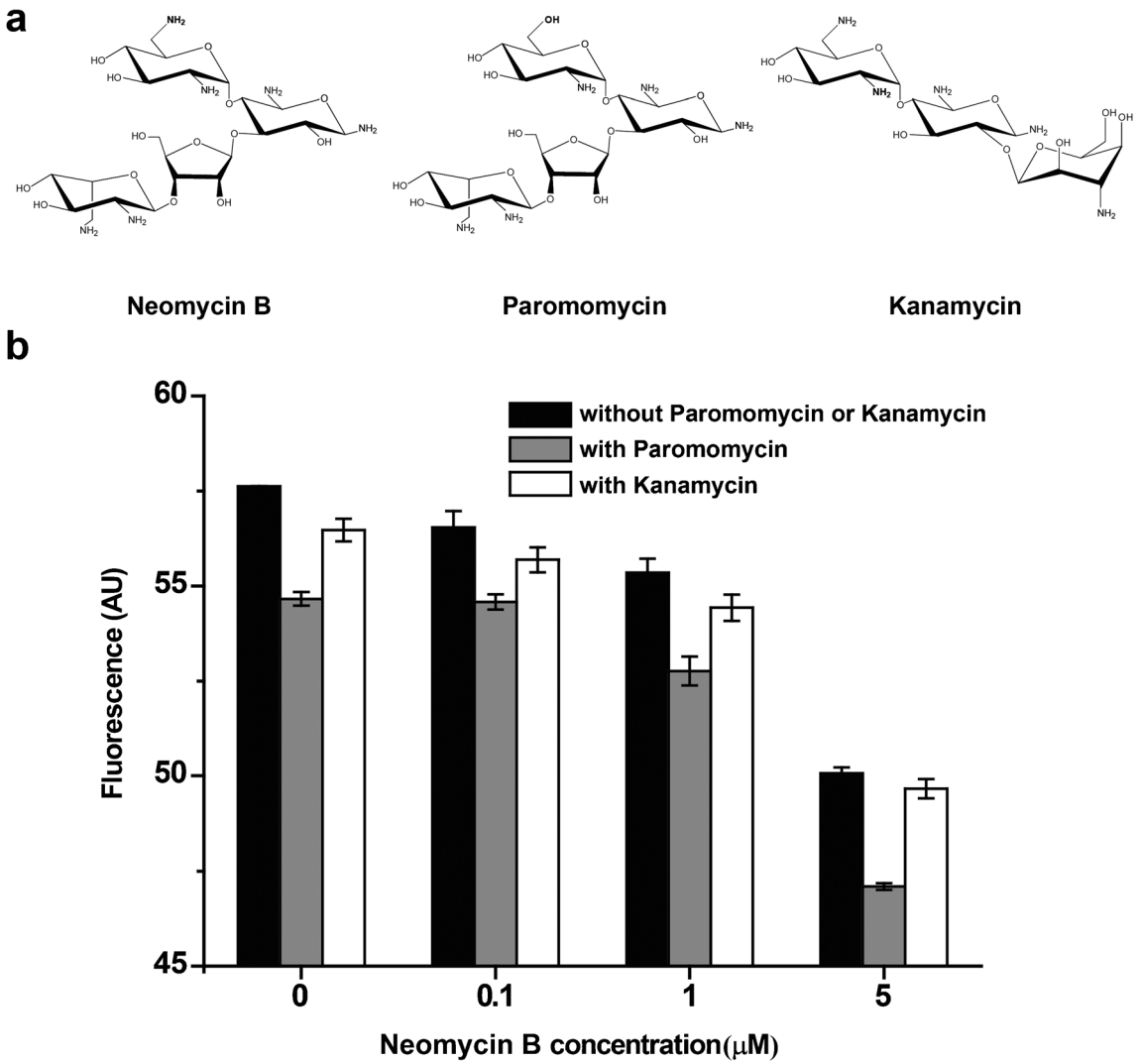

Fig. 2 Selectivity of the Neomycin B aptasensor. **a** The chemical structures of Neomycin B, Paromomycin, and Kanamycin. **b** Changes in fluorescence intensity following the addition of different concentrations of Neomycin B with or without Paromomycin (10 μM) or Kanamycin (10 μM). Data represent mean values and standard deviations from triplicate experiments

samples provided the required concentrations of Na^+, Mg^{2+}, and other ions, and the stable and moderate pH environment (pH 7.4) to the conformational changes of the RNA aptamer upon binding of Neomycin B [11, 27]. Figure 1b represents the linear relationship between the fluorescence intensity (518 nm) and Neomycin B concentration (from 0.1 to 10 μM). The detection limit ($3\sigma/S$, in which σ is the standard deviation for the blank solution, $n = 8$, and S is the slope of the calibration curve) was 0.01 μM.

Paromomycin and Kanamycin are Neomycin class-aminoglycosides, which both possess the essential neamine moiety (Fig. 2a) [8]. Specifically, Paromomycin only differs from Neomycin B in the substitution of a single amino group with a hydroxyl group. Furthermore, the aptamers evolved against these aminoglycosides have similar structures [28]. Therefore, cross reactivity with the neamine-containing aminoglycosides (Paromomycin and Kanamycin) was tested in order to evaluate the specificity of the aptasensor. Figure 2b shows the fluorescence intensity (518 nm) of the sensor solutions containing Neomycin B (from 0 to 5 μM) with or without 10 μM Paromomycin and Kanamycin. After adding 10 μM Paromomycin, no more than 7 % signal interference was detected in Neomycin B samples. Following the addition of 10 μM Kanamycin, the signal interference decreased to 2 %. The possible reason for the interference is the high structure similarity between Paromomycin and Neomycin B.

It is well known that the intrinsic instability of RNA against endonucleases precludes the application of RNA aptamers in biological fluids. In this study, split RNA fragments and RNA-modified AuNPs increased the stability of the RNA aptasensor in milk. RNase I is an endoribonuclease that preferentially hydrolyzes single-stranded RNA to nucleoside 3′-monophosphates via nucleoside 2′-,3′-cyclic monophosphate, which is usually used to remove RNA from DNA solutions. Figure 3a shows the changes in the fluorescence intensity of the 5′-FAM-labeled NEO1 attached AuNPs treated with or without RNase I over 720 min. The fluorescence intensity increased slightly with time, because very few RNA sequences were degraded and released from the AuNPs. Figure 3b, c illustrates the absorption spectra of the supernatants of NEO1-AuNP conjugates incubated with and without RNase I over time (720 min). The absorption (260 nm) of nucleic acid increased slightly with time, due to increased amounts of biodegraded or released oligonucleotides from the conjugates. Taken together,

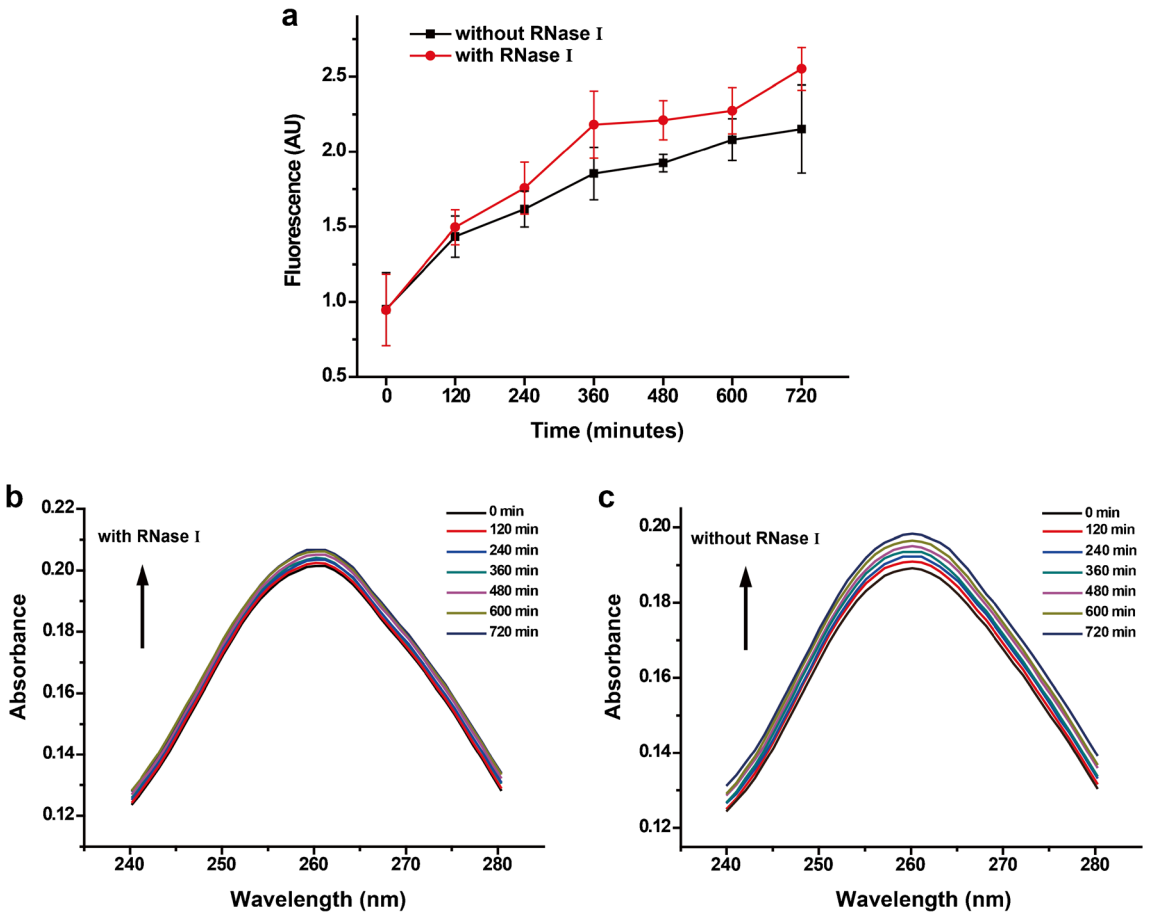

Fig. 3 RNase inhibition of RNA-modified AuNPs. **a** Fluorescence intensities (518 nm) of 5′-FAM-labeled NEO1-AuNP conjugates treated without (*black*) and with (*red*) RNase I over 720 min. Data represent mean values and standard deviations from triplicate experiments. Absorption spectra of the supernatants of NEO1-AuNP conjugates incubated with (**b**) and without (**c**) RNase I over time (0 to 720 min)

although there were minor differences in the fluorescence intensities and the absorption values (260 nm) between the two groups, these results established that most attached oligonucleotides (NEO1) were indeed present on the AuNPs after incubation with RNase I. Ribonuclease activity can be inhibited by RNA-modified AuNPs during the detection process. The reason is attributed to that most nucleases are inhibited by the high local salt concentration around the nanoparticle surface [26]. In this aptasensor design, AuNPs not only acted as fluorescence quenchers but also enhanced the biostability of the attached RNA fragments.

Conclusion

In summary, we developed a novel self-assembling RNA aptamer-based nanoparticle sensor for the detection of Neomycin B in milk, whose design can be easily tailored to other small molecules for various diagnostic and analytical applications. Splitting the RNA aptamer into two shorter half fragments at the site outside of the ligand-binding pocket does not affect the binding properties of the aptamer. One fragment (NEO1) was conjugated to AuNPs via the quick adsorption of a polyA tail. The other fragment (NEO2) was labeled with a fluorophore (FAM). The two individual fragments self-assembled in the presence of the ligand. Upon ligand binding, the fragments came into close proximity, resulting in fluorescence quenching. This RNA aptasensor exhibited a low detection limit (0.01 μM) and good selectivity toward Neomycin B, without chemical modification of the RNA sequence. Specifically, because of the shorter RNA fragments and the nuclease inhibition ability of the RNA-modified AuNPs, the RNA sequences remained stable during the experiments. Therefore, this work will serve as an example for the development of novel biosensors based on RNA aptamers for the detection of attractive biological targets.

Acknowledgments We are grateful for the financial support from the National Natural Science Foundation of China (81502589), the Natural Science Foundation of Guangdong Province, China (2014A030310481), and The Science and Technology Project of Shenzhen (CXZZ20130515092016300, 201302017).

Compliance with ethical standards

Conflict of interest The authors declare that they have no conflict of interest.

References

1. Hermann T, Patel DJ. Adaptive recognition by nucleic acid aptamers. Science. 2000;287:820–5.
2. Liu J, Cao Z, Lu Y. Functional nucleic acid sensors. Chem Rev. 2009;109:1948–98.
3. Song S, Wang L, Li J, et al. Aptamer-based biosensors. TrAC Trends Anal Chem. 2008;27:108–17.
4. Ferguson BS, Hoggarth DA, Maliniak D, et al. Real-time, aptamer-based tracking of circulating therapeutic agents in living animals. Sci Transl Med. 2013;5:213ra165.
5. Liu J, Lu Y. Fast colorimetric sensing of adenosine and cocaine based on a general sensor design involving aptamers and nanoparticles. Angew Chem Int Ed. 2005;45:90–4.
6. Brumbt A, Ravelet C, Grosset C, et al. Chiral stationary phase based on a biostable L-RNA aptamer. Anal Chem. 2005;77:1993–8.
7. Sun H, Zhu X, Lu PY, et al. Oligonucleotide aptamers: new tools for targeted cancer therapy. Mol Ther Nucleic Acids. 2014;3:e182.
8. De-los-Santos-Álvarez N, Lobo-Castañón MJ, Miranda-Ordieres AJ, Tuñón-Blanco P. Modified-RNA aptamer-based sensor for competitive impedimetric assay of neomycin B. J Am Chem Soc. 2007;129:3808–9.
9. Forster C, Zydek M, Rothkegel M, et al. Properties of an LNA-modified ricin RNA aptamer. Biochem Biophys Res Commun. 2012;419:60–5.
10. Ruta J, Ravelet C, Grosset C, et al. Enantiomeric separation using an L-RNA aptamer as chiral additive in partial-filling capillary electrophoresis. Anal Chem. 2006;78:3032–9.
11. Wallis MG, von Ahsen U, Schroeder R, Famulok M. A novel RNA motif for neomycin recognition. Chem Biol. 1995;2:543–52.
12. Jin Y, Jang J-W, Lee M-H, Han C-H. Development of ELISA and immunochromatographic assay for the detection of neomycin. Clin Chim Acta. 2006;364:260–6.
13. Lian W, Liu S, Yu J, et al. Electrochemical sensor using neomycin-imprinted film as recognition element based on chitosan-silver nanoparticles/graphene-multiwalled carbon nanotubes composites modified electrode. Biosens Bioelectron. 2013;44:70–6.
14. De-los-Santos-Álvarez N, Lobo-Castañón MJ, Miranda-Ordieres AJ, Tuñón-Blanco P. SPR sensing of small molecules with modified RNA aptamers: detection of neomycin B. Biosens Bioelectron. 2009;24:2547–53.
15. Hill HD, Mirkin CA. The bio-barcode assay for the detection of protein and nucleic acid targets using DTT-induced ligand exchange. Nat Protoc. 2006;1:324–36.
16. Jin R, Wu G, Li Z, et al. What controls the melting properties of DNA-linked gold nanoparticle assemblies? J Am Chem Soc. 2003;125:1643–54.
17. Jiang H, Ling K, Tao X, Zhang Q. Theophylline detection in serum using a self-assembling RNA aptamer-based gold nanoparticle sensor. Biosens Bioelectron. 2015;70:299–303.
18. Pei H, Li F, Wan Y, et al. Designed diblock oligonucleotide for the synthesis of spatially isolated and highly hybridizable functionalization of DNA-gold nanoparticle nanoconjugates. J Am Chem Soc. 2012;134:11876–9.
19. Frazao C, McVey CE, Amblar M, et al. Unravelling the dynamics of RNA degradation by ribonuclease II and its RNA-bound complex. Nature. 2006;443:110–4.
20. Ilgu M, Fulton DB, Yennamalli RM, et al. An adaptable pentaloop defines a robust neomycin-B RNA aptamer with conditional ligand-bound structures. RNA. 2014;20:815–24.
21. Jiang L, Majumdar A, Hu W, et al. Saccharide-RNA recognition in a complex formed between neomycin B and an RNA aptamer. Structure. 1999;7:817–27.
22. Zhang X, Liu B, Servos MR, Liu J. Polarity control for nonthiolated DNA adsorption onto gold nanoparticles. Langmuir. 2013;29:6091–8.
23. Rouge JL, Hao L, Wu XA, et al. Spherical nucleic acids as a divergent platform for synthesizing RNA-nanoparticle conjugates through enzymatic ligation. ACS Nano. 2014;8:8837–43.

24. Li W, Dong Y, Wang X, et al. PolyA-tailed and fluorophore-labeled aptamer-gold nanoparticle conjugate for fluorescence turn-on bioassay using iodide-induced ligand displacement. Biosens Bioelectron. 2015;66:43–9.
25. Zhang X, Liu B, Dave N, et al. Instantaneous attachment of an ultrahigh density of nonthiolated DNA to gold nanoparticles and its applications. Langmuir. 2012;28:17053–60.
26. Seferos DS, Prigodich AE, Giljohann DA, et al. Polyvalent DNA nanoparticle conjugates stabilize nucleic acids. Nano Lett. 2009;9:308–11.
27. Stampfl S, Lempradl A, Koehler G, Schroeder R. Monovalent ion dependence of neomycin B binding to an RNA aptamer characterized by spectroscopic methods. ChemBioChem. 2007;8:1137–45.
28. Hermann T, Westhof E. RNA as a drug target: chemical, modelling, and evolutionary tools. Curr Opin Biotechnol. 1998;9:66–73.